Gazi Üniversitesi
Fen Bilimleri Dergisi
PART C: TASARIM VE TEKNOLOJİ

Gazi University
Journal of Science
PART C: DESIGN AND TECHNOLOGY

GU J Sci, Part C, 14(1): 528-544 (2026)

EEG and ECG Microstructure Markers During Apnea Transition Phases in Central and Obstructive Sleep Apnea

Onur KOÇAK[1-2*], Ziya TELATAR[1]

[1]*Başkent University, Engineering Faculty, Department of Biomedical Engineering, Ankara, Türkiye*
[2]*Başkent University, Engineering Faculty, Department of Computer Engineering, Ankara, Türkiye*

Article Info

Research article
Received: 06/12/2026
Revision: 27/02/2026
Accepted: 03/03/2026

Keywords

Sleep apnea
EEG and ECG microstructure markers
HRV
pulse transit time
apnea transitions
spectral analysis

Makale Bilgisi

Araştırma makalesi
Başvuru: 06/12/2026
Düzeltme: 27/02/2026
Kabul: 03/03/2026

Anahtar Kelimeler

Uyku apnesi,
EEG ve EKG mikroyapısal belirteçler,
Kalp hızı değişkenliği,
Nabız geçiş zamanı,
Apne geçişleri,
Spektral analiz

Graphical/Tabular Abstract (Grafik Özet)

This study characterizes EEG and ECG microstructural markers during apnea transitions in CSA and OSA using signal processing. Findings reveal distinct cortical stability and autonomic dynamics, aiding phenotype differentiation and clinical diagnosis. / Bu çalışma, sinyal işleme teknikleriyle CSA ve OSA'da apne geçişlerindeki EEG ve EKG mikroyapı belirteçlerini tanımlamaktadır. Bulgular, apne fenotiplerinin ayrımına ve klinik tanıya katkı sağlayan farklı kortikal stabilite ve otonomik dinamikler ortaya koymaktadır.

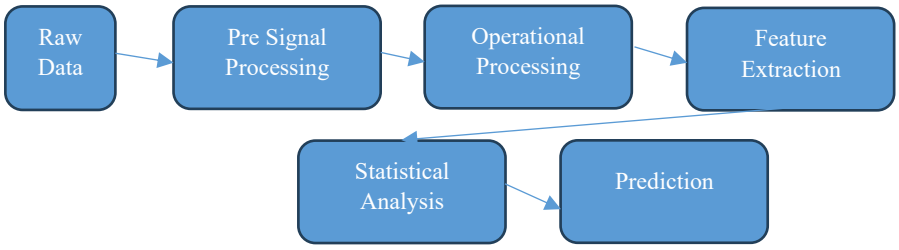

Figure A: *Signal processing stages and event-based segmentation for sleep apnea microstructure analysis. /* ***Şekil A:*** *Uyku apnesi mikroyapı analizi için sinyal işleme aşamaları ve olay tabanlı bölütleme.*

Highlights (Önemli noktalar)

- *Distinct electrophysiological/autonomic differences exist between CSA and OSA during apnea transitions. / CSA ve OSA arasında apne geçişlerinde belirgin elektrofizyolojik ve otonomik farklar saptanmıştır.*
- *Increased EEG power and shortened PTT in CSA indicate rapid autonomic/cortical responses. / CSA'da artan EEG gücü ve kısalan PTT, hızlı otonomik ve kortikal yanıtları işaret etmektedir.*
- *Wake-like intrusions in OSA reflect lower cortical stability compared to CSA. / OSA'daki uyanıklık benzeri intrüzyonlar, CSA'ya kıyasla daha düşük kortikal stabiliteyi yansıtmaktadır.*
- *EEG markers and PTT are robust parameters for differentiating apnea phenotypes. / EEG belirteçleri ve PTT, apne fenotiplerini ayırt etmede güçlü parametrelerdir.*

Aim (Amaç): *The study identifies EEG/ECG microstructure markers during apnea in CSA/OSA and examines trends by sleep stage and severity. / Çalışmada CSA/OSA apne geçişlerinde EEG/EKG mikroyapı belirteçlerinin tanımlanması ve uyku evresi/şiddetine göre trendlerin incelenmesi amaçlanmıştır.*

Originality (Özgünlük): *This research offers a unique comparative analysis of invisible microstructure markers in CSA and OSA using biomedical engineering techniques. / Bu araştırma, biyomedikal mühendisliği teknikleriyle CSA ve OSA'daki görünmeyen mikroyapı belirteçlerinin özgün bir karşılaştırmalı analizini sunmaktadır.*

Results (Bulgular): *Polysomnography records of 32 male patients (16 CSA, 16 OSA) were retrospectively analyzed, revealing significant differences in EEG sub-band energies, PTT, and LF/HF ratios across apnea transitions. While CSA showed higher cortical stability, OSA exhibited increased arousal-like activity and distinct autonomic shifts. / Toplam 32 erkek hastaya (16 CSA, 16 OSA) ait polisomnografi kayıtları geriye dönük olarak analiz edilmiş; apne geçişlerinde EEG alt bant enerjileri, PTT ve LF/HF oranlarında anlamlı farklılıklar saptanmıştır. CSA'da daha yüksek kortikal stabilite, OSA'da ise artmış uyanıklık benzeri aktivite ve belirgin otonomik değişimler gözlenmiştir.*

Conclusion (Sonuç): *Quantitative EEG and PTT markers are robust tools for clinical monitoring and differentiating apnea phenotypes. / Kantitatif EEG ve PTT belirteçleri, apne fenotiplerinin ayrımı ve klinik izlem için güçlü araçlardır.*

*Corresponding author, e-mail: okocak@baskent.edu.tr
DOI: 10.29109/gujsc.1837129

GU J Sci, Part C, 14(1): 528-544 (2026)

Gazi Üniversitesi
Fen Bilimleri Dergisi
PART C: TASARIM VE TEKNOLOJİ

Gazi University
Journal of Science
PART C: DESIGN AND TECHNOLOGY

http://dergipark.gov.tr/gujsc

EEG and ECG Microstructure Markers During Apnea Transition Phases in Central and Obstructive Sleep Apnea

Onur KOÇAK[1-2*], Ziya TELATAR[1]

[1]*Başkent University, Engineering Faculty, Department of Biomedical Engineering, Ankara, Türkiye*
[2]*Başkent University, Engineering Faculty, Department of Computer Engineering, Ankara, Türkiye*

Article Info

Research article
Received: 06/12/2026
Revision: 27/02/2026
Accepted: 03/03/2026

Keywords

Sleep apnea
EEG and ECG microstructure markers
HRV
pulse transit time
apnea transitions
spectral analysis

Abstract

This study aimed to characterize EEG- and ECG-derived microstructural (MS) markers during apnea transitions in central sleep apnea (CSA) and obstructive sleep apnea (OSA), and to examine how these transient dynamics vary across sleep stages and apnea severity. Polysomnography data from 32 male patients (16 CSA, 16 OSA) were retrospectively analyzed. EEG sub-band energies (delta, theta, alpha, beta), pulse transit time (PTT), Hjorth parameters, and frequency-domain HRV (LF/HF) were computed for pre-apnea, intra-apnea, and post-apnea epochs. Patients were further stratified according to AHI severity. Group comparisons were performed using parametric and non-parametric tests with Bonferroni adjustment. OSA and CSA demonstrated distinct electrophysiological patterns. CSA showed increasing EEG sub-band power and decreasing PTT from pre- to intra-apnea, indicating rapid autonomic adjustment with suggesting relatively preserved cortical stability. OSA exhibited reduced EEG power, lengthened PTT, and transition-dependent modulation in beta-band activity during apnea, consistent with arousal-like intrusions. Stage-specific analysis revealed that revealed notable transition-related differences, marked by delta–theta enhancement and alpha–beta suppression. In N2 and N3, delta activity showed characteristic divergence across apnea intervals, suggesting stage-dependent microstructural (MS) responses within each stage. High-resolution EEG and ECG features provide complementary insights into the physiological mechanisms distinguishing OSA from CSA. EEG microstructures (MS) captured transient cortical dynamics not visible in conventional scoring, suggesting their potential value as early biomarkers of respiratory instability. These findings may support improved diagnostic accuracy and individualized management strategies in sleep apnea.

Merkezi ve Obstrüktif Uyku Apnesinde Apne Geçiş Evrelerinde EEG ve EKG Mikroyapı Belirteçleri

Makale Bilgisi

Araştırma makalesi
Başvuru: 06/12/2026
Düzeltme: 27/02/2026
Kabul: 03/03/2026

Anahtar Kelimeler

Uyku apnesi,
EEG ve EKG mikroyapısal belirteçler,
Kalp hızı değişkenliği,
Nabız geçiş zamanı,
Apne geçişleri,
Spektral analiz

Öz

Bu çalışma, santral uyku apnesi (CSA) ve obstrüktif uyku apnesi (OSA) sırasında apne geçişleri boyunca EEG ve EKG'den türetilen mikroyapısal belirteçleri tanımlamayı ve bu geçici dinamiklerin uyku evreleri ile apne şiddetine göre nasıl değiştiğini incelemeyi amaçlamıştır. Toplam 32 erkek hastaya (16 CSA, 16 OSA) ait polisomnografi kayıtları geriye dönük olarak analiz edilmiştir. Pre-apne, intra-apne ve post-apne epokları için EEG alt bant enerjileri (delta, teta, alfa, beta), nabız geçiş zamanı (PTT), Hjorth parametreleri ve frekans alanı kalp hızı değişkenliği (LF/HF) değerleri hesaplanmıştır. Hastalar ayrıca AHI şiddetine göre sınıflandırılmıştır. Grup karşılaştırmaları parametrik ve parametrik olmayan testler kullanılarak Bonferroni düzeltmesi ile gerçekleştirilmiştir. OSA ve CSA arasında belirgin elektrofizyolojik farklılıklar gözlenmiştir. CSA grubunda pre-apneden intra-apneye geçişte EEG alt bant güçlerinde artış ve PTT'de azalma saptanmış olup, bu durum hızlı otonom yanıtlarla birlikte göreceli olarak korunmuş kortikal stabiliteyi düşündürmektedir. OSA grubunda ise EEG gücünde azalma, PTT'de uzama ve apne sırasında beta bant aktivitesinde geçişe bağlı değişimler gözlenmiş; bu bulgular uyanıklık benzeri intrüzyonlarla uyumlu bulunmuştur. Evreye özgü analizler, özellikle REM uykusunda belirgin geçiş ilişkili farklılıklar olduğunu ve delta–teta artışı ile alfa–beta baskılanmasının öne çıktığını göstermiştir. N2 ve N3 evrelerinde delta aktivitesi apne aralıkları boyunca karakteristik farklılaşmalar göstererek evreye özgü mikroyapısal yanıtları işaret etmiştir. Yüksek çözünürlüklü EEG ve EKG özellikleri, OSA ve CSA'yı ayırt eden fizyolojik mekanizmalar hakkında tamamlayıcı bilgiler sunmaktadır. EEG mikroyapıları, geleneksel skorlamada görünmeyen geçici kortikal dinamikleri yakalayarak solunumsal instabilitenin erken biyobelirteçleri olma potansiyeli göstermektedir. Bu bulgular, uyku apnesinde tanısal doğruluğun artırılmasına ve bireyselleştirilmiş tedavi yaklaşımlarının desteklenmesine katkı sağlayabilir.

*Corresponding author, e-mail: okocak@baskent.edu.tr
DOI: 10.29109/gujsc.1837129

1. INTRODUCTION (GİRİŞ)

Breathing disturbances during sleep are associated with systemic physiological impairment and increased cardiovascular, neurological, and metabolic risk [1-4]. Sleep apnea is marked by recurrent reductions or cessations in ventilation that induce hypoxemia or brief cortical arousals detectable in the EEG [5,6].

Clinically, it is classified into obstructive sleep apnea (OSA), central sleep apnea (CSA), and mixed sleep apnea (MSA) although the present study focuses on OSA and CSA. OSA involves persistent inspiratory effort against a collapsed upper airway, CSA reflects loss of both airflow and respiratory drive, and MSA represents a transition from central to obstructive patterns within a single respiratory cycle [7,8].

Digital physiological signals—especially electrocardiography (ECG) and electroencephalography (EEG)—are central tools for characterizing sleep-disordered breathing [9,10]. Prior studies have examined RR-interval variability, heart rate variability (HRV), and spectral EEG markers for apnea detection and sleep staging [11-15]. Reductions in theta-band power correlate with increasing apnea severity, while multimodal oxygen saturation–EEG analyses have demonstrated high clinical diagnostic performance [16,17]. Frequency-domain work using FFT further indicates that waveform duration shifts parallel changes in power distribution [18].

Another major focus has been arousal identification to understand how respiratory instability influences autonomic and cortical responses during PSG [19]. Advanced decomposition techniques with adaptive time–frequency resolution reveal hierarchical EEG dynamics beyond conventional linear spectral analysis [20]. Multichannel recordings improve sensitivity for transient cortical fluctuations in deeper non-REM sleep, and stage-dependent EEG signatures have been linked to nocturnal oxygenation changes [21,22]. EEG MS features have also been associated with neurobehavioral resilience and cognitive vulnerability in untreated OSA [23,24]. Additional studies report that respiratory instability interacts with ocular movement patterns and cardiac rhythm complexity, both correlating with apnea severity [22-27].

Sleep fragmentation studies highlight phase-A3 frequency as a marker of MS instability and daytime somnolence [28]. Oscillatory mapping of respiratory-related arousals suggests that sensorimotor cortical recruitment varies by sleep stage and apnea load, independent of autonomic reactivity [29]. Machine-learning frameworks using multimodal PSG channels have recently achieved high-accuracy automated staging through optimized 30-second feature extraction [30].

Despite these advances, most work has analyzed EEG or ECG independently and not at the precise temporal boundaries where apnea disrupts physiological continuity.

Moreover, sleep-transition micro dynamics across multiple sleep stages have not been jointly modeled with synchronized multimodal metrics.

To address these gaps, the present study characterizes neuro-cardiac signatures at pre-apnea, apnea, and post-apnea intervals across N1, N2, N3, and REM sleep by integrating spectral EEG profiles with ECG-based temporal and frequency descriptors. Here, MS refer to latent cortical response patterns not visually discernible in short raw segments but detectable through quantitative segmentation and higher-order statistical analysis. By jointly modeling these dynamics, the study aims to identify early biomarkers of respiratory instability to support more efficient clinical decision-making and improve patient outcomes.

The manuscript is organized as follows: Section 2 details the methodology and analytical pipeline, Section 3 presents empirical findings, and Section 4 discusses key interpretations and future implications.

2. MATERIALS AND METHODS (MATERYAL VE METOD)

2.1. Participants (Katılımcılar)

This retrospective study included 32 male participants (mean age 42 ± 9 years) diagnosed with sleep-disordered breathing. Sixteen participants met the criteria for obstructive sleep apnea (OSA) and sixteen for central sleep apnea (CSA). All subjects were evaluated at the Sleep Disorders Diagnosis and Treatment Unit of the Department of Thoracic Diseases, Diskapi Yildirim Beyazit Training and Research Hospital (Ankara, Türkiye).

Participants were categorized by Apnea–Hypopnea Index (AHI) severity into four groups: <5, 5–<15, 15–<30, and ≥30 events/hour (n = 4 patients per AHI subgroup). The mean body mass index (BMI) was 30 ± 7 kg/m², with no significant demographic differences between OSA and CSA groups.

2.2. Procedure (Prosedür)

Overnight polysomnography (PSG) was performed using standard clinical protocols, recording EEG,

ECG, oronasal airflow via thermistor, respiratory effort, and peripheral oxygen saturation [31,32]. The Apnea–Hypopnea Index (AHI) was used as the primary clinical parameter, representing the hourly frequency of apnea–hypopnea events.

All recordings were obtained using a Compumedics E-Series™ system and scored with ProFusion 3™ software by a certified sleep technologist in accordance with international guidelines. EEG signals were collected from F4, C4, and O2 electrodes (10–20 system); ECG from a three-lead configuration; respiratory effort via nasal thermistor and thoracoabdominal belts; and oxygen saturation via pulse oximetry. All channels were sampled at 256 Hz, with a 50 Hz notch filter applied to suppress power-line interference [33].

The study protocol was reviewed and authorized by the clinical director of the sleep center. All procedures complied with institutional and national ethical regulations, and written informed consent was obtained from each participant for the use of anonymized data.

Continuous PSG recordings were segmented into 30-second epochs and categorized into three event-related windows: pre-apnea (30 s before onset), intra-apnea (during the event), and post-apnea (30 s after termination) [33]. Only epochs scored as sleep were included in the analysis. *Total Sleep Time (TST)* was defined as the cumulative duration of scored sleep epochs. The *Apnea–Hypopnea Index (AHI)* was computed as Eq. (2.1) :

$$AHI = \frac{N_{apnea} + N_{hypopnea}}{TST_{(hours)}} \tag{2.1}$$

2.3. Signal Preprocessing (Sinyal İşleme)

All PSG signals were preprocessed using a unified MATLAB workflow to maintain strict temporal synchronization across modalities. For EEG and ECG, DC offset was removed using a moving-average filter, followed by zero-phase Butterworth band-pass filtering (BPF) (0.5–45 Hz for EEG; 0.5–40 Hz for ECG) to eliminate slow drifts and high-frequency noise while preserving physiological content [34]. Respiratory effort and oxygen saturation signals were denoised with a 5-Hz low-pass filter (LPF) to minimize motion artifacts without distorting respiratory patterns. The original sampling rate was preserved for all channels, and artifact-related distortions were addressed during feature-specific processing steps rather than by rejecting epochs, ensuring that the full structure of apnea events remained intact.

2.4. Apnea Segmentation and Epoch Definition (Apne Bölütleme ve Epok Tanımı)

Apnea events were identified using physician-scored polysomnography (PSG) annotations in accordance with standard clinical scoring procedures. Signal analyses were performed based on conventional 30-second PSG epochs. Rather than analyzing variable-duration apnea intervals directly, the intra-apnea segment was defined as the fixed 30-second epoch containing the scored apnea event. The pre-apnea and post-apnea segments corresponded to the immediately preceding and subsequent 30-second epochs, respectively. Consequently, all analyzed segments (pre-, intra-, and post-apnea) had identical temporal lengths, ensuring consistency in subsequent spectral analyses.

In patients with lower AHI ranges (AHI 0–5 and 5–15), consecutive apnea occurrences leading to temporal overlap or aliasing effects were not observed in either CSA or OSA groups. In a limited subset of patients with higher disease severity (AHI 15–30 and particularly AHI > 30), consecutive or overlapping apnea episodes were occasionally present. To preserve temporal independence between analyzed transitions and to avoid biased spectral estimation, sequential apnea episodes without sufficient recovery intervals were excluded from analysis under clinical supervision. These events were considered unsuitable for transition-based microstructural evaluation.

Following this filtering procedure, only isolated apnea transitions were retained. For each selected apnea event, one intra-apnea epoch together with one pre-apnea and one post-apnea epoch were included in the analysis. This approach ensured non-overlapping temporal windows and comparable physiological transition segments across subjects while minimizing temporal dependency between consecutive events.

2.5. Feature Extraction (Öznitelik Çıkarımı)

ECG Signal Processing (EKG Sinyal İşleme)

ECG morphology varies with heart-rate dynamics and fluctuations in arterial oxygen saturation, both commonly influenced by sleep apnea [35]. PTT the delay between the ECG R-wave and the arrival of the corresponding peripheral pulse was derived from synchronized ECG, PSG, and pulse-oximetry

signals [36]. As an indirect marker of upper-airway resistance and arousal burden, PTT provides physiologically relevant information during apnea-related desaturation [37].

The analytical workflow used for ECG spectral estimation is presented in Figure 1. As an initial signal preprocessing step, a Moving Average Filter (MAF) was applied to the ECG signal. Subsequently, an initial detection of R-waves was performed by computing the mean value of the signal within a predefined sliding window template followed by the application of the Teager Energy operator to emphasize abrupt amplitude variations. This procedure enhanced the prominence and visibility of R-peaks.

Thereafter, in order to determine the final set of R-peak events, 30% of the computed signal value was selected as an adaptive threshold, and peaks exceeding this threshold were identified and marked. Finally, to quantitatively assess changes in sympathetic and parasympathetic modulation across the pre-apnea, intra-apnea, and post-apnea periods, the Yule–Walker spectral decomposition technique—one of the most widely used parametric methods in the literature—was employed.

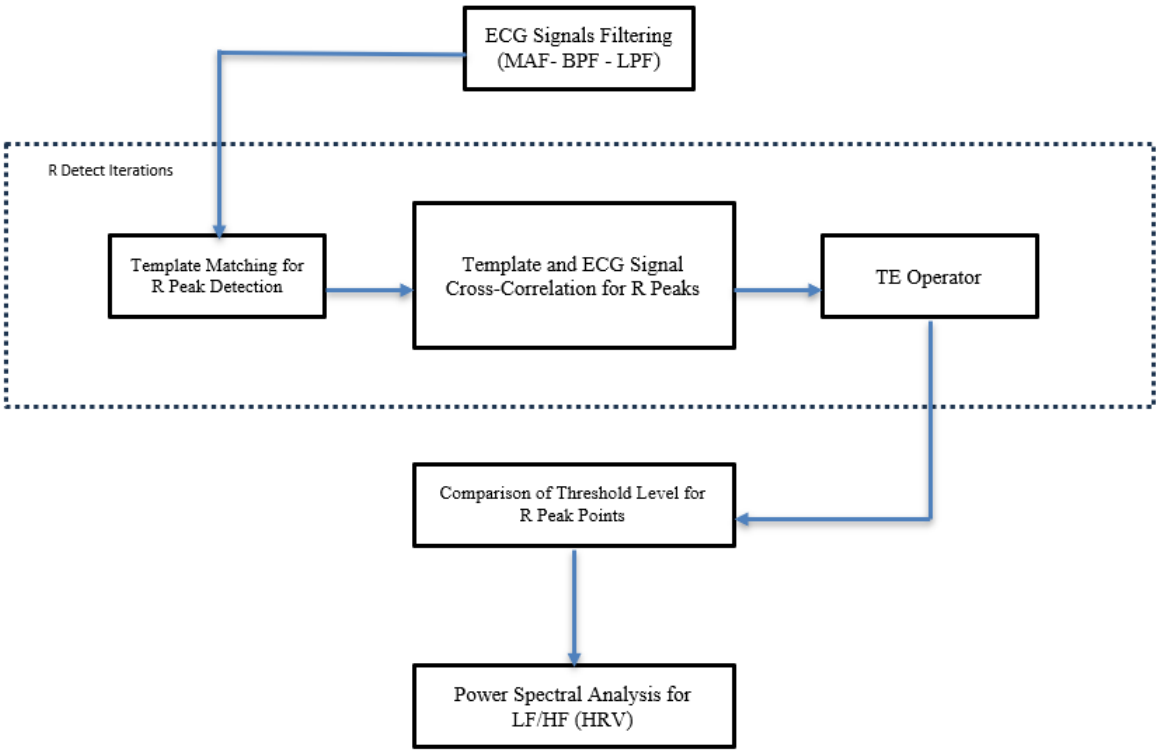

Figure 1. ECG Signal Processing Steps (EKG Sinyal İşleme Adımları)

Frequency Domain Analysis of ECG Signals (EKG Sinyallerinde Frekans Bölgesi Analizi)

For frequency-domain characterization of the HRV signal, two complementary spectral estimation approaches were employed for distinct analytical purposes.

R-wave identification was performed using a correlation-based detection scheme in which segments of the ECG signal were compared with a representative template waveform. For this purpose, a template extracted from a clean portion of the ECG was selected, and the similarity between each ECG signal segment and the template waveform was quantified using a normalized cross-correlation (NCC) function, which provides a scale-invariant measure of morphological similarity [38]. In Eq. (2.2), $\boldsymbol{f_i}$ denotes the $\boldsymbol{i}$-th sample of the ECG signal segment and $\boldsymbol{t_i}$ represents the corresponding $\boldsymbol{i}$-th sample of the template waveform, while $\boldsymbol{N}$ corresponds to the number of samples within the analysis window. The terms $\boldsymbol{\mu_f}$ and $\boldsymbol{\mu_t}$indicate the mean values of the ECG segment and the template waveform, respectively. This formulation yields a dimensionless similarity metric bounded between −1 and +1, facilitating robust R-wave enhancement.

$$\boldsymbol{NCC} = \frac{\sum_{i=1}^{N}(\boldsymbol{f_i} - \boldsymbol{\mu_f})(\boldsymbol{t_i} - \boldsymbol{\mu_t})}{\sqrt{\sum_{i=1}^{N}(\boldsymbol{f_i} - \boldsymbol{\mu_f})^2 \sum_{i=1}^{N}(\boldsymbol{t_i} - \boldsymbol{\mu_t})^2}} \quad (2.2)$$

To further emphasize abrupt morphological variations around the R-wave, the Teager Energy (TE) operator was applied to the ECG signal. This nonlinear operator is sensitive to instantaneous changes in both amplitude and frequency components, thereby enhancing transient features associated with R-peak morphology. In the discrete-time formulation given in Eq. (2.3), $\boldsymbol{x[n]}$ denotes the ECG signal sample at time index $\boldsymbol{n}$, and $\boldsymbol{\Psi_x[n]}$ represents the corresponding Teager Energy output.

$$\boldsymbol{\Psi_x[n] = x^2[n] - x[n+1]x[n-1]} \tag{2.3}$$

Following TE processing, a thresholding step was conducted to isolate R-wave candidates. The mean amplitude within a sliding analysis window was computed, and 30% of this mean value was adopted as the adaptive threshold for event detection [40,41].

For frequency-domain characterization of the resulting HRV series, an autoregressive (AR) modeling approach based on the Yule–Walker equations were employed [42,43]. This parametric method permits high-resolution estimation of the HRV power spectrum, even for relatively short data segments. The resulting HRV spectral density distribution is demonstrated in Figure 2.

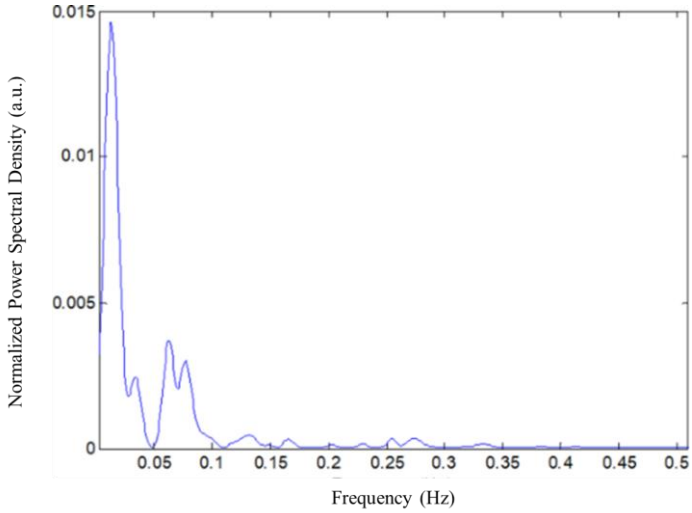

Figure 2. HRV Frequency Spectrum VLF<0.04Hz, LF between 0.04Hz – 0.15Hz, HF between 0.15Hz – 0.4Hz (HRV Frekans Spektrumu: VLF < 0,04 Hz, LF 0,04 Hz – 0,15 Hz arası, HF 0,15 Hz – 0,4 Hz arası)

For frequency-domain characterization of the HRV signal, complementary spectral estimation approaches were employed for distinct analytical purposes. An autoregressive (AR) modeling framework based on the Yule–Walker equations was first applied to obtain a high-resolution representation of the HRV spectral distribution, particularly suitable for relatively short analysis segments. This parametric estimation was primarily used to visualize spectral structure and support qualitative assessment of autonomic dynamics.

Quantitative extraction of standard HRV frequency-domain indices was subsequently performed using Welch's power spectral density method (Hamming window, 50% overlap). Spectral power was calculated within conventional frequency bands: VLF (0.003–0.04 Hz), LF (0.04–0.15 Hz), and HF (0.15–0.40 Hz). Thus, AR modeling and Welch estimation were used for complementary purposes rather than redundant spectral calculations. Autonomic regulation was represented as at Eq. (2.4):

$$LF/_{HF} = \frac{P_{LF}}{P_{HF}} \tag{2.4}$$

Time Domain Analysis of ECG Signals (EKG Sinyallerinde Zaman Bölgesi Analizi)

Temporal characteristics of heart rate variability (HRV) were quantified using Hjorth's descriptor set—activity, mobility, and complexity—which is well suited for the analysis of non-stationary biomedical signals [44,45]. Hjorth activity corresponds to the variance of the signal, denoted as $\boldsymbol{\sigma_x^2}$, and reflects the overall amplitude dispersion.

Hjorth mobility ($\boldsymbol{M_x}$) characterizes the mean frequency or rate of change of the signal and is defined as the square root of the ratio between the variance of the first derivative of the signal and the variance of the original signal, as given in Eq. (2.5):

$$M_x = \sqrt{\frac{\sigma^2{}_{x'}}{\sigma^2{}_x}} \tag{2.5}$$

The third parameter, Hjorth complexity (C_x), describes the degree to which the signal deviates from a pure sinusoidal waveform. It quantifies the relative variation between the second and first derivatives of the signal, normalized by mobility. In this study, Hjorth complexity (C_x) is referred to as FF for consistency with ECG-based temporal descriptors. This measure is defined in Eq. (2.6):

$$C_x = \frac{M_{x'}}{M_x} = \frac{\sigma_{x''}/\sigma_{x'}}{\sigma_{x'}/\sigma_x} \tag{2.6}$$

Together, these Hjorth parameters provide a compact yet effective representation of both instantaneous variance and rapid temporal fluctuations in the HRV signal, thereby capturing its temporal complexity and dynamical behavior [46,47].

EEG Signal Processing (EEG Sinyal İşleme)

EEG signals (10–100 μV) reflect neural oscillations across delta (<4 Hz), theta (4–8 Hz), alpha (8–13 Hz), and beta (13–30 Hz) bands [48]. These rhythms support conventional sleep staging and are sensitive to cortical arousals and fragmentation. Because respiratory disturbances alter cortical activity, changes in EEG spectral composition provide a useful marker of apnea-related neural responses [49].

In accordance with standard clinical polysomnography conventions implemented in Philips and Compumedics clinical analysis software, the beta frequency band was defined within the 13–30 Hz range. Although a broader band-pass filtering range extending to 45 Hz was applied during preprocessing to ensure signal stability and minimize boundary effects, spectral power calculations were strictly limited to the canonical beta-band limits. Frequencies above 30 Hz were not included in feature extraction or statistical analyses.

Spectral analysis was performed using established estimation frameworks. Given the brief and rapid nature of apnea-related transitions, the Yule–Walker AR method was selected for spectral estimation due to its robustness with short segments. Each 30-second EEG epoch was divided into overlapping 64-sample windows (50% overlap), enabling fine-scale tracking of pre-apnea, intra-apnea, and post-apnea fluctuations. Spectral power within canonical EEG bands was computed for each window, and participant-specific transitions were analyzed across all 32 subjects. This approach allowed precise characterization of cortical dynamics surrounding apnea events [50-53].

2.6 Statistical Analysis (İstatistiksel Analiz)

In this study, apnea transition periods (pre-apnea, intra-apnea, and post-apnea) were identified at the event level based on physician-scored apnea epochs. For each apnea event, the intra-apnea epoch and its adjacent epochs were used to define the pre- and post-apnea segments, and EEG and ECG features were extracted accordingly.

Although feature extraction was performed at the event level to capture microstructural physiological transitions, statistical analyses were conducted at the patient level to avoid treating multiple apnea events from the same subject as independent observations. Specifically, for each patient, features obtained from all detected apnea events were aggregated by calculating within-patient mean values for each condition and feature. Consequently, each patient contributed a single aggregated value per feature and condition to the statistical comparisons.

Group-level statistical tests were therefore performed using patient-level aggregated data (OSA: n = 16; CSA: n = 16). AHI subgroup analyses were also based on patient-level aggregation (n = 4 per subgroup), and results derived from these subgroups were interpreted cautiously due to the limited sample size. This hierarchical approach ensured that the statistical unit of analysis remained patient rather than individual apnea events.

All statistical analyses were performed to evaluate differences in EEG- and ECG-derived features across apnea types and apnea- related time segments. Comparisons between OSA and CSA groups were conducted using the student's t-test or Mann–Whitney U test, depending on normality and variance assumptions. Differences among three or more groups were evaluated using one-way analysis of variance (ANOVA) when parametric assumptions were satisfied. When normality or homogeneity assumptions were not met, the Kruskal–Wallis test was applied. For statistically significant omnibus results, pairwise comparisons

were performed using Bonferroni-adjusted post-hoc tests. Within-subject differences across temporal states (pre-apnea, intra-apnea, post-apnea) were examined using paired t-tests for normally distributed variables and Wilcoxon signed-rank tests for non-parametric data. Associations between continuous variables were assessed using Spearman's rank correlation. All tests were two-tailed, and statistical significance was set at $p < 0.05$.Each patient was treated as the independent statistical unit in all inferential analyses. This procedure minimized temporal dependency between consecutive events and ensured comparable spectral estimation across apnea transitions. Statistical analyses were performed using standard scientific computing software, and all assumptions were verified prior to hypothesis testing. The overall analytical workflow of the study is summarized in Figure 3.

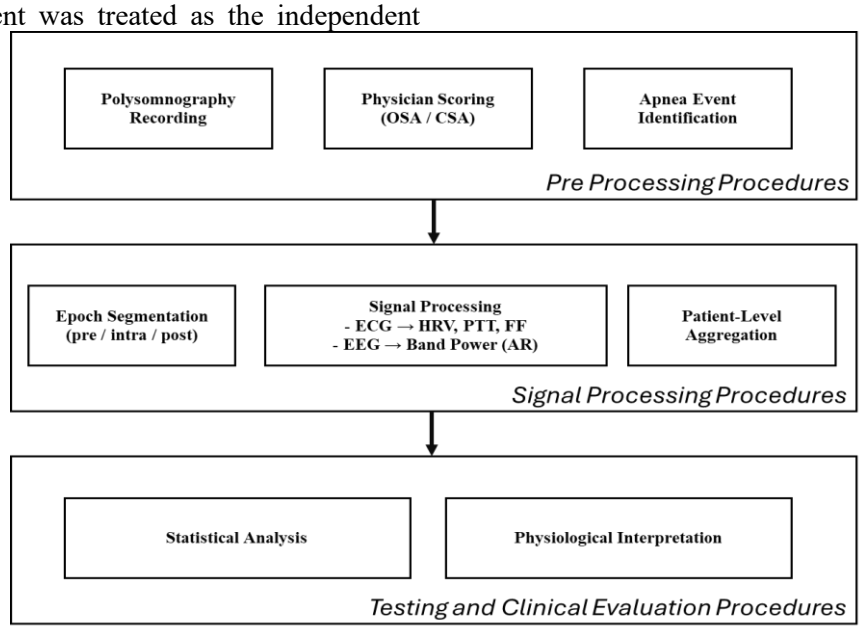

Figure 3. Analytical Workflow of the study. (Çalışmanın Analitik İş Akışı)

3. RESULTS AND DISCUSSION (SONUÇ VE TARTIŞMA)

This study analyzed PSG recordings from 16 OSA and 16 CSA patients, with each group further divided into four AHI-based subgroups (n = 4). The classification strategy and signal-processing workflow are summarized in Figure 4.

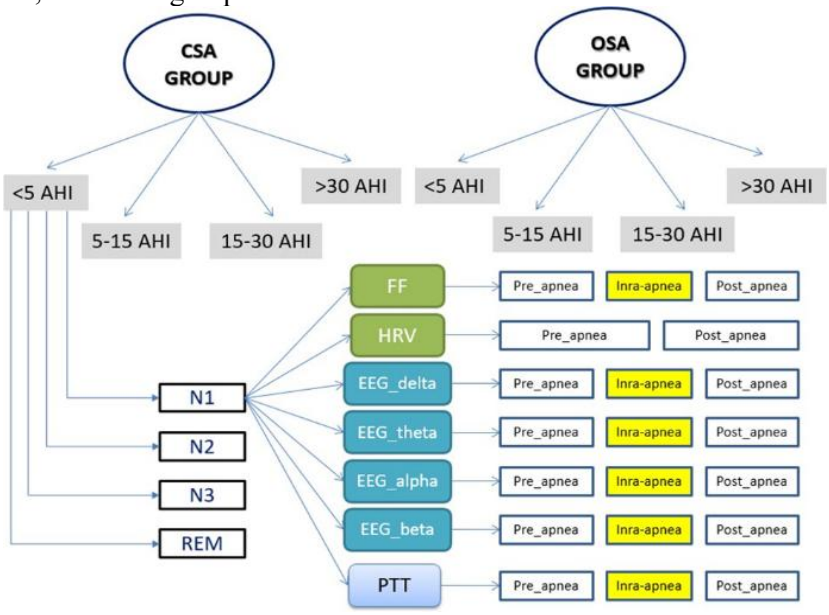

Figure 4. Analytical workflow illustrating apnea-event segmentation and synchronized EEG–ECG signal processing. (Apne-olay segmentasyonunu ve senkronize EEG–ECG sinyal işlemeyi resmeden analitik iş akışı)

OSA and CSA groups, stratified by AHI severity, were evaluated across all apnea-transition stages. EEG sub-band power was assessed for each participant during pre-apnea, intra-apnea, and post-apnea periods to identify MS alterations not visible in raw recordings. Parallel analyses of PTT and Hjorth Form Factor (FF) were performed on ECG signals. The main findings are summarized in Table 1.

Table 1. Patient-level comparison of EEG and ECG features between OSA and CSA groups across pre-apnea, intra-apnea, and post-apnea periods (mean ± SD). Statistical significance was assessed using the Mann–Whitney U test. (Tablo 1. OSA ve CSA grupları arasında apne öncesi, apne sırası ve apne sonrası dönemlerdeki EEG ve EKG özniteliklerinin hasta düzeyinde karşılaştırılması (ortalama ± SS). İstatistiksel analiz Mann–Whitney U testi kullanılarak değerlendirilmiştir.)

Apnoea Group		***BMI***	***Age***	***Pre_FF***	***Apne_FF***	***Post_FF***
CSA	*Mean ± Std. Deviation*	*30,08 ± 4,91*	*38,44 ± 10,5*	*3,75 ± 1,82*	*3,76 ± 1,90*	*3,84 ± 1,97*
	Median (min–max)	*29,15*	*37,00*	*4,15*	*4,36*	*4,16*
OSA	*Mean ± Std. Deviation*	*29,28 ± 6,32*	*46,06 ± 7,069*	*2,01 ± 1,22*	*1,88 ± 0,99*	*1,89 ± 1,012*
	Median (min–max)	*28,10*	*45,00*	*1,54*	*1,51*	*1,49*
P				***0,001***	***0,001***	***0,001***

Apnoea Transition		***Pre Apnea***			
Apnoea Group		***EEG_delta***	***EEG_teta***	***EEG_alfa***	***EEG_beta***
CSA	*Mean ± Std. Deviation*	*1,49E+06 ± 3,13E+06*	*3,57E+05 ± 650512,1*	*3,93E+04 ± 99416,9*	*2,27E+04 ± 70073,6*
	Median (min–max)	*4,02E+05*	*1,08E+05*	*1,83E+04*	*5,41E+03*
OSA	*Mean ± Std. Deviation*	*2,13E+06 ± 10421650,29*	*3,94E+05 ± 1778154,05*	*1,27E+04 ± 9328,9*	*5,85E+03 ± 8115,2*
	Median (min–max)	*2,10E+05*	*7,04E+04*	*1,11E+04*	*3,61E+03*
P		***0,019***	***0,012***	***0,030***	***0,066 (n.s.)***

Apnoea Transition		***Intra Apnea***			
Apnoea Group		***EEG_delta***	***EEG_teta***	***EEG_alfa***	***EEG_beta***
CSA	*Mean ± Std. Deviation*	*3,79E+06 ± 7099873,8*	*7,90E+05 ± 1349413,5*	*4,72E+04 ± 126794,26*	*2,75E+04 ± 92366,61*
	Median (min–max)	*5,48E+05*	*1,68E+05*	*1,59E+04*	*7,22E+03*
OSA	*Mean ± Std. Deviation*	*7,41E+05 ± 1879671,42*	*1,59E+05 ± 333025,19*	*1,12E+04 ± 5460,16*	*4,95E+03 ± 6727,66*
	Median (min–max)	*1,78E+05*	*5,65E+04*	*1,18E+04*	*3,38E+03*
P		***0,012***	***0,004***	***0,001***	***0,005***

Apnoea Transition		***Post Apnea***			
Apnoea Group		***EEG_delta***	***EEG_teta***	***EEG_alfa***	***EEG_beta***
CSA	*Mean ± Std. Deviation*	*8,95E+05 ± 1748636,38*	*2,27E+05 ± 381687,3*	*3,94E+04 ± 121059,63*	*2,26E+04 ± 85458,68*
	Median (min–max)	*3,39E+05*	*9,59E+04*	*1,29E+04*	*3,21E+03*
OSA	*Mean ± Std. Deviation*	*1,20E+06 ± 2899349,188*	*2,56E+05 ± 563387,97*	*1,31E+04 ± 9728,94*	*8,77E+03 ± 14012,15*
	Median (min–max)	*2,80E+05*	*8,26E+04*	*1,08E+04*	*4,11E+03*
P		***0,489 (n.s.)***	***0,402 (n.s.)***	***0,096 (n.s.)***	***0,301 (n.s.)***

Apnoea Group		***Pre_PTT***	***Apne_PTT***	***Post_PTT***
CSA	*Mean ± Std. Deviation*	*475,83 ± 217,52*	*325,34 ± 70,41*	*315,14 ± 43,17*
	Median (min–max)	*364,00*	*312,00*	*308,00*
OSA	*Mean ± Std. Deviation*	*317,79 ± 43,66*	*381,70 ± 203,77*	*325,34 ± 99,61*
	Median (min–max)	*309,00*	*325,33*	*309,80*
P		***0,001***	***0,005***	***0,411 (n.s.)***

Values represent patient-level aggregated means calculated after within-patient averaging across apnea events. P-values correspond to between-group comparisons performed using the Mann–Whitney U test. Statistical significance was defined as $p < 0.05$.

Table 1 presents patient-level comparisons of EEG- and ECG-derived features between CSA and OSA groups across pre-apnea, intra-apnea, and post-apnea periods. Several parameters, including post-apnea EEG features, pre-apnea beta-band activity, and post-apnea PTT values, did not demonstrate statistically significant between-group differences; however, these findings are reported to provide a complete and unbiased representation of apnea-transition dynamics. Values are presented as patient-level aggregated means (± SD), calculated after within-patient averaging across apnea events.

In CSA patients, FF values exhibited a gradual increase from pre- to post-apnea, whereas OSA patients showed their highest FF values before apnea onset.

Pre-apnea delta power was significantly lower in CSA compared with OSA, consistent with higher delta-band activity in the OSA group prior to apnea events. CSA patients demonstrated higher theta and alpha power, indicating relatively increased low-frequency spectral activity during the pre-apnea period.

As shown in Table 1, Beta-band activity did not show statistically significant differences during the pre-apnea period ($p = 0.066$). However, significant between-group differences emerged during the intra-apnea interval ($p = 0.005$). From pre- to intra-apnea, beta-band power decreased in OSA patients, whereas CSA patients demonstrated an opposite trend characterized by increased beta activity. This divergence may indicate differing cortical response patterns associated with apnea events in the two diagnostic groups.

Post-apnea PTT differences were not statistically significant but are included for completeness of reporting. Significant differences between OSA and CSA were observed during pre-apnea and intra-apnea periods. Whereas PTT remained relatively stable in CSA, it increased during apnea in OSA patients, indicating prolonged peripheral pulse arrival time.

Figure 5. illustrates the variations in heart rate variability (HRV) across sleep stages (NI, NII, NIII, and REM), apnea types (CSA and OSA), and apnea–hypopnea index (AHI) severity groups. A graphical representation was preferred over tabular presentation in order to more effectively capture and interpret dynamic HRV changes across different physiological conditions.

Figure 5.a. shows HRV variations during the pre- and post-apnea periods across sleep stages. A reduction in HRV following apnea events is observed during lighter sleep stages, such as NI and NII, as well as during REM sleep, which is characterized by increased cortical activity and rapid eye movements. In contrast, during deep sleep (NIII), an increase in the LF/HF ratio is evident.

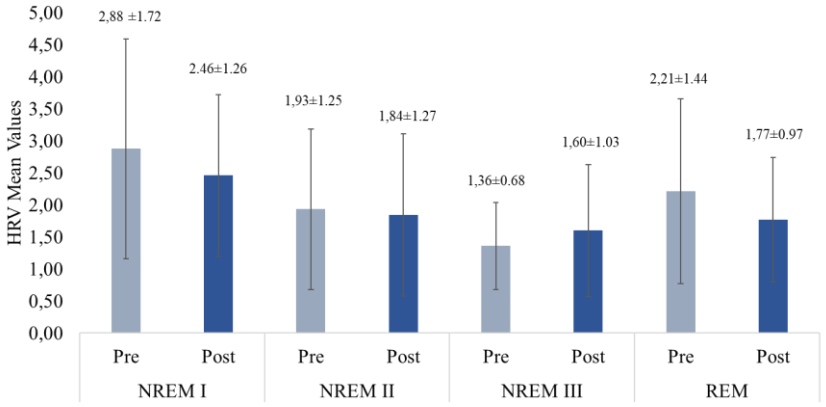

Figure 5.a. HRV Differences Apnea Transition for Sleep Stages (Uyku Evrelerine Göre Apne Geçişlerinde HRV Farklılıkları)

The post-apnea reduction in the LF/HF ratio during lighter sleep stages and REM sleep may be attributed to a relative dominance of parasympathetic activity following the apnea event. This decrease in LF/HF ratio during these stages is suggestive of a limited arousal-related response of the central nervous system following apnea termination. Conversely, the observed increase in sympathetic modulation during NIII sleep reflects enhanced autonomic activation, which may facilitate central nervous system arousal or transition to a lighter sleep stage in response to respiratory disturbance.

Figure 5.b. illustrates the changes in HRV values across apnea–hypopnea index (AHI) severity groups during the transition from pre- to post-apnea periods. With the exception of the AHI > 30 group, a consistent decrease in HRV is observed across all severity categories. Overall, HRV demonstrates a decreasing trend following apnea termination, indicating a shift in autonomic regulation during the post-apnea period.

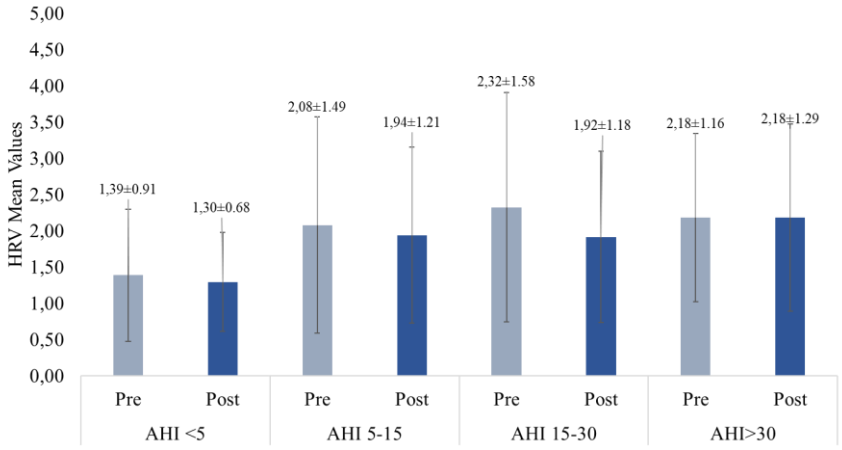

Figure 5.b. HRV Differences Apnea Transition for AHI (AHI Şiddetine Göre Apne Geçişlerinde HRV Farklılıkları)

Figure 5.c. shows the changes in HRV values during the transition from pre-apnea to post-apnea periods in patients with OSA and CSA. A decrease in HRV is observed in both apnea types following apnea termination. However, the magnitude of this reduction is proportionally greater in OSA patients. This finding suggests a more pronounced autonomic response to apnea events in OSA, potentially reflecting heightened sympathetic activity during the pre-apnea period and a more rapid engagement of central autonomic regulatory mechanisms compared to CSA.

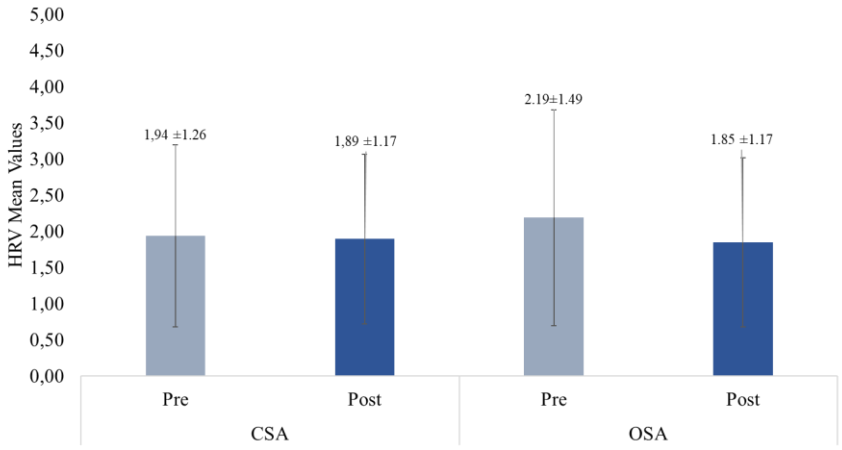

Figure 5.c. HRV Differences Apnea Transition for Apnea Types (Apne Türlerine Göre Apne Geçişlerinde HRV Farklılıkları)

Significant differences across AHI-based severity groups were primarily driven by PTT values, while most EEG sub-band comparisons did not reach statistical significance (Table 2). Pre-apnea PTT decreased significantly with AHI severity ($p < 0.05$). Significant PTT differences persisted during intra-apnea, while non-significant EEG sub-band trends are included for a comprehensive overview of transition dynamics.

Table 2. Patient-level comparison of EEG sub-band power and pulse transit time (PTT) across AHI severity groups during pre-apnea, intra-apnea, and post-apnea transitions. (Apne öncesi, apne sırası ve apne sonrası geçiş evrelerinde AHI grupları arasında EEG alt bant gücü ve nabız geçiş zamanının (PTT) hasta düzeyinde karşılaştırılması)

Apnoea Transition		***Pre Apnea***				
AHI Group		***EEG_delta***	***EEG_teta***	***EEG_alfa***	***EEG_beta***	***PTT***
AHI <5	*Mean ± Std. Deviation*	*3,97E+05 ± 688095,34*	*1,09E+05 ± 166306,049*	*1,25E+04 ± 7803,9*	*6,18E+03 ± 8061,9*	*464,94 ± 236,4*
	Median (min–max)	*1,00E+05*	*3,10E+04*	*1,01E+04*	*3,25E+03*	*337,50*
AHI 5-15	*Mean ± Std. Deviation*	*4,37E+06 ± 13867213,5*	*8,22E+05 ± 2399427,5*	*2,02E+04 ± 14065,73*	*7,89E+03 ± 9508,77*	*457,37 ± 218,41*
	Median (min–max)	*3,32E+05*	*9,26E+04*	*1,44E+04*	*4,58E+03*	*335,00*
AHI 15-30	*Mean ± Std. Deviation*	*9,30E+05 ± 1765170,41*	*2,57E+05 ± 424148,7*	*5,69E+04 ± 141129,4*	*3,53E+04 ± 99288,59*	*370,97 ± 156,58*
	Median (min–max)	*3,30E+05*	*9,14E+04*	*1,55E+04*	*5,12E+03*	*314,42*
AHI>30	*Mean ± Std. Deviation*	*1,22E+06 ± 2156572,48*	*2,75E+05 ± 417215,24*	*1,68E+04 ± 11204,64*	*9,00E+03 ± 9807,33*	*369,35 ± 121,6*
	Median (min–max)	*4,02E+05*	*1,06E+05*	*1,31E+04*	*± 5672,09*	*312,00*
P		***0,102 (n.s.)***	***0,142 (n.s.)***	***0,326 (n.s.)***	***0,174 (n.s.)***	***0,017***

Apnoea Transition		***Intra Apnea***				
AHI Group		***EEG_delta***	***EEG_teta***	***EEG_alfa***	***EEG_beta***	***PTT***
AHI <5	*Mean ± Std. Deviation*	*1,55E+06 ± 3524162,57*	*3,23E+05 ± 650580,77*	*1,41E+04 ± 6705,13*	*4,86E+03 ± 3295,8*	*447,67 ± 299,5*
	Median (min–max)	*1,46E+05*	*4,97E+04*	*1,33E+04*	*3,66E+03*	*324,00*
AHI 5-15	*Mean ± Std. Deviation*	*1,31E+06 ± 2508376,44*	*2,99E+05 ± 518497,96*	*1,65E+04 ± 9853,71*	*7,40E+03 ± 7338,58*	*346,64 ± 64,96*
	Median (min–max)	*2,62E+05*	*7,75E+04*	*1,29E+04*	*3,25E+03*	*330,14*
AHI 15-30	*Mean ± Std. Deviation*	*2,09E+06 ± 5197918,78*	*4,72E+05 ± 1062230,91*	*6,90E+04 ± 180336,7*	*4,49E+04 ± 131200,66*	*325,50 ± 37,54*
	Median (min–max)	*1,95E+05*	*6,40E+04*	*1,36E+04*	*4,57E+03*	*317,75*
AHI>30	*Mean ± Std. Deviation*	*4,77E+06 ± 8645811,23*	*9,38E+05 ± 1601728,91*	*2,09E+04 ± 16019,01*	*9,32E+03 ± 8640,68*	*304,40 ± 12,02*
	Median (min–max)	*9,03E+05*	*1,84E+05*	*1,26E+04*	*7,30E+03*	*308,00*
P		***0,036***	***0,080 (n.s.)***	***0,947 (n.s.)***	***0,213 (n.s.)***	***0,001***

Apnoea Transition		***Post Apnea***				
AHI Group		***EEG_delta***	***EEG_teta***	***EEG_alfa***	***EEG_beta***	***PTT***
AHI <5	*Mean ± Std. Deviation*	7,74E+05 ± 1741680,71	1,80E+05 ± 342738,08	1,23E+04 ± 6108,4	4,70E+03 ± 3259,53	314,98 ± 49,03
	Median (min–max)	2,80E+05	8,29E+04	1,27E+04	3,12E+03	312,00
AHI 5-15	*Mean ± Std. Deviation*	6,98E+05 ± 1345055,75	1,68E+05 ± 268122,68	1,33E+04 ± 6277,51	4,89E+03 ± 5821,31	345,82 ± 124,34
	Median (min–max)	3,64E+05	1,01E+05	1,23E+04	3,12E+03	317,14
AHI 15-30	*Mean ± Std. Deviation*	1,95E+06 ± 3617253,38	4,45E+05 ± 728661,77	6,78E+04 ± 170567,22	4,46E+04 ± 120412,73	323,09 ± 48,94
	Median (min–max)	2,11E+05	6,80E+04	1,45E+04	4,16E+03	310,33
AHI>30	*Mean ± Std. Deviation*	5,22E+05 ± 1001195,2	1,31E+05 ± 206462,57	1,25E+04 ± 5937,92	7,43E+03 ± 10266,74	294,72 ± 11,49
	Median (min–max)	3,03E+05	7,74E+04	1,16E+04	4,38E+03	295,36
P		***0,920 (n.s.)***	***0,924 (n.s.)***	***0,658 (n.s.)***	***0,516 (n.s.)***	***0,001***

Values represent patient-level aggregated statistics calculated after within-patient averaging across apnea events. Both statistically significant and non-significant findings are reported to ensure complete and unbiased representation of apnea-transition analyses.

When evaluated across AHI categories, delta-band power showed higher values in groups with greater apnea severity, while theta, alpha, and beta-band activities exhibited variable patterns without consistent statistical differences. These findings suggest that apnea severity is more strongly associated with slow-wave activity and cardiovascular timing alterations than with higher-frequency EEG components. Post-apnea comparisons did not reveal statistically significant differences across AHI groups despite observable numerical variations.

P-values represent comparisons across AHI severity groups using one-way ANOVA or Kruskal–Wallis tests depending on distributional assumptions, followed by Bonferroni-corrected post-hoc analyses when applicable.

The distinction between OSA and CSA became more apparent during analyses focused on apnea-transition periods. Comparisons of spectral characteristics revealed clear differences between the two conditions, particularly during the transition from pre-apnea to intra-apnea stages. Percentage-based analysis demonstrated opposing physiological responses between groups (Table 3). In CSA patients, EEG sub-band power increased across all frequency ranges during apnea onset, whereas OSA patients exhibited reductions in spectral activity over the same transition interval.

Table 3. Pre-to-intra apnea transition changes of EEG sub-band power, Hjorth Form Factor, and pulse transit time (PTT) in CSA and OSA groups.(CSA ve OSA Gruplarında Apne Öncesinden Apne Sırasına Geçişte EEG Alt Bant Gücü, Hjorth Form Faktörü ve Nabız Geçiş Zamanı (PTT) Değişimleri)

Pre - Intra Apne Transient Changes	***Delta***	***Teta***	***Alfa***	***Beta***	***FF***	***PTT***
CSA	*+ 36,31 %*	*+ 55,54 %*	*+ 20,11 %*	*+ 33,46 %*	*+ 4,31 %*	*- 31,63 %*
OSA	*- 24,15 %*	*- 19,74 %*	*- 11,81 %*	*- 6,37 %*	*- 6,55 %*	*+ 20,11 %*

To further quantify these transition dynamics, percentage changes between pre-apnea and intra-apnea periods were calculated (Table 3). Detailed percentage analysis further confirmed these opposing physiological responses between CSA and OSA groups. In CSA patients, EEG sub-band power increased across all frequency ranges, with delta, theta, alpha, and beta activity rising by 36.3%, 55.5%, 20.1%, and 33.5%, respectively. In contrast, OSA patients demonstrated reductions across all EEG frequency bands during the same transition interval. A similar divergence was observed in Hjorth Form Factor values, which increased modestly in CSA (+4.3%) but decreased in OSA (−6.5%). Pulse transit time (PTT) exhibited the opposite behavior between groups, decreasing in CSA (−31.6%) while increasing in OSA (+20.1%). These opposing percentage changes indicate fundamentally different neurocardiac adjustment mechanisms during the transition into apnea (pre-to-intra interval) in central versus obstructive sleep apnea.

Supporting these findings, statistically significant differences in PTT were detected in CSA patients during both pre-apnea ($p < 0.001$) and intra-apnea ($p < 0.005$) periods (Table 1).

Although not all EEG comparisons reached statistical significance, the observed patterns were retained to provide a comprehensive representation of transition-related physiological dynamics.

Table 4 summarizes the relative intra- to pre-apnea spectral shifts across sleep stages. REM sleep demonstrated the most distinct modulation. Although REM is typically dominated by theta and alpha rhythms31, intra-apnea periods showed substantial increases in delta and theta power, accompanied by marked reductions in alpha and beta activity. Despite the lower overall frequency of apnea events in REM due to heightened cortical activation, these findings suggest that respiratory disturbances still provoke a coordinated Central Nervous System (CNS) response.

Table 4 outlines the magnitude of the upward and downward shifts in EEG activity. The reductions in delta and theta power during N2 were relatively small compared with the pronounced increases observed in N1 and N3.

Table 4. Intra_apnea / pre_apnea transition rate of change (Apne öncesinden apne sırasına geçişteki değişim oranı)

Intra / Pre Apnea Transient Ratio	*Delta*	*Theta*	*Alpha*	*Beta*
N1	*2,12*	*1,96*	*1,11*	*1,16*
N2	*0,77*	*0,84*	*1,04*	*1,03*
N3	*2,05*	*1,8*	*1,37*	*1,56*
REM	*4,72*	*2,83*	*0,87*	*0,59*

A similar pattern was observed in REM sleep, where delta and theta power increased during pre- and intra-apnea intervals. This likely reflects an adaptive neural response in which the brain suppresses alpha and beta activity to preserve sleep continuity despite respiratory disturbances. Although the magnitude of these changes varied with apnea severity, the overall pattern suggests that compensatory mechanisms remain active during REM-related events.

Dingli et al. [16] reported increases in alpha, beta, and delta activity using 10-second windows. We observed a 23% reduction in alpha energy and a 41% reduction in beta energy during apnea. These values rebounded in the post-apnea interval, while delta power—showing a marked intra- to pre-apnea increase—returned toward baseline. Theta activity followed a similar pattern: a prominent intra-apnea increase that normalized post-apnea. REM therefore showed the most abrupt electrophysiological fluctuations, suggesting rapid MS adjustments not visible in raw EEG but detectable through transient spectral shifts.

Stage-specific variability was also evident in N2 sleep. Delta and theta power declined during pre- and intra-apnea and continued into the post-apnea interval. Alpha and beta activity initially increased at apnea onset but fell below baseline afterward, reflecting the transitional nature of N2 between lighter and deeper sleep. N1 showed a drop-in delta activity post-apnea, while N3 exhibited a robust pre- to intra-apnea rise in delta power, consistent with slow-wave dominance; post-apnea delta remained the largest component of the EEG spectrum.

In summary, cortical responses to apnea differed markedly across sleep stages. Cardiac measures showed minimal stage-dependent variation ($p > 0.005$), whereas EEG features revealed rapid, event-specific modulation. N1 and N3 displayed clear spectral fluctuations across transition periods, but REM showed the most complex profile, with distinct alpha–beta suppression and delta–theta enhancement. These findings provide a technical basis for refined EEG analysis and highlight the MS neural dynamics underlying apnea events, particularly in N2 and REM sleep.

4. CONCLUSION (SONUÇLAR)

This study demonstrated that obstructive and central sleep apnea exhibit distinct neurocardiac signatures during pre-apnea, intra-apnea, and post-apnea transitions. CSA was characterized by increasing EEG sub-band activity and shorter PTT during apnea, reflecting rapid autonomic adjustments suggesting relatively preserved cortical stability during apnea. In contrast, OSA showed reductions in EEG power, lengthening of PTT, and more pronounced arousal-like features, indicating predominantly mechanically mediated respiratory obstruction accompanied by stronger cardiocortical involvement.

Across sleep stages, EEG markers revealed clear stage-dependent fluctuations, whereas cardiac measures remained relatively stable. REM sleep showed the most dynamic cortical responses, with marked shifts in delta–theta and alpha–beta activity during apnea. Event-level analyses also uncovered transient EEG MS that were not evident in broader sleep-stage comparisons, underscoring the importance of high-resolution temporal approaches in sleep research.

Taken together, the integrated EEG and ECG features identified in this study provide complementary physiological markers that may assist in differentiating OSA and CSA and highlight early physiological indicators that may support improved diagnosis and individualized treatment strategies.

Future studies integrating larger cohorts and real-time analytical pipelines may help translate these multimodal markers into clinically applicable decision-support tools.

LIMITATIONS (KISITLAR)

This study has several limitations that should be considered when interpreting the findings. The sleep recordings analyzed in this study were obtained from the Sleep Disorders Center of the Department of Pulmonary Diseases at Dışkapı Yıldırım Beyazıt Training and Research Hospital. All recordings were acquired using a Compumedics E Series system (Sydney, Australia) and processed with ProFusion 3 software. Sleep staging and event scoring were performed by a certified sleep technician in accordance with the AASM 2007 guidelines.

A total of 32 patients diagnosed with obstructive sleep apnea (OSA) or central sleep apnea (CSA) were included in the study. For each apnea–hypopnea index (AHI) severity category, polysomnography recordings of four patients, each lasting between 6 and 8 hours, were analyzed, corresponding to a total of 26,880 epochs across all subjects. The relatively small sample size within individual AHI subgroups may limit statistical power and should be considered when interpreting subgroup-level findings.

The study population consisted exclusively of male patients. Female participants were not included in order to minimize potential variability related to hormonal influences on sleep physiology. While this approach reduced biological variability, it also limits the generalizability of the findings to the broader sleep apnea population.

All participants were admitted to the clinic following approval by the Department of Pulmonary Diseases, and written informed consent was obtained prior to data acquisition. The dataset used in this study was anonymized by the clinical staff and retrospectively analyzed for scientific purposes. Because the dataset was previously collected under institutional clinical authorization and fully anonymized prior to analysis, additional ethics committee approval was not required according to institutional regulations. The same dataset and ethical statement were previously reported in a study published in paper [54].

Although the dataset overlaps with our previously published work, the scientific objectives and analytical frameworks of the two studies differ substantially. Accordingly, no data reuse occurred at the level of analytical outcomes or reported results. The earlier study primarily focused on general sleep-related signal characteristics and global physiological assessments across sleep recordings. In contrast, the present study introduces an event-centered analytical framework specifically designed to investigate microstructural EEG–ECG interactions during apnea transition periods. By incorporating pre-apnea, intra-apnea, and post-apnea segmentation together with integrated cortical and cardiovascular markers, the current work provides a distinct physiological interpretation and novel insights into transition dynamics that were not addressed in the previous publication.

Feature extraction in this study was based on the analysis of ECG and EEG signals. Unlike our previous investigations, EEG analysis was limited to signals recorded from the F4, C4, and O2 electrodes, as selected and scored by a physician. While this approach enabled focused microstructural analysis, it restricted the spatial resolution of EEG-derived spectral interpretations and represents an additional limitation of the study. Future studies incorporating higher-density EEG montages may help clarify spatially distributed cortical dynamics during apnea transitions.

ACKNOWLEDGEMENTS (TEŞEKKÜR)

The authors would like to thank Prof. Dr. Hikmet Fırat, Prof. Dr. Sadık Ardıç and Prof. Dr. Osmar Eroğul for their invaluable guidance, feedback, and supervisory support throughout the study.

DECLARATION OF ETHICAL STANDARDS
(ETİK STANDARTLARIN BEYANI)

The author of this article declares that the study protocol was reviewed and authorized by the clinical director of the sleep center. All procedures complied with institutional and national ethical regulations, and written informed consent was obtained from each participant for the use of anonymized data.

Bu makalenin yazarları, çalışma protokolünün uyku merkezinin klinik sorumlusu tarafından incelenip onaylandığını beyan eder. Tüm prosedürler kurumsal ve ulusal etik kurallara uygun

olarak gerçekleştirilmiş olup, anonimleştirilmiş verilerin kullanımı için her katılımcıdan yazılı bilgilendirilmiş onam alınmıştır.

AUTHORS' CONTRIBUTIONS (YAZARLARIN KATKILARI)

Onur KOÇAK: This author was involved in the collection, anonymisation and processing of data for this study.

Yazar , çalışmada verilerin toplanması, anonimleştirilmesi ve işlenmesi çalışmasında yer almıştır.

Ziya TELATAR: The author has statistically interpreted and evaluated the data obtained in the study.

Yazar, çalışmada elde edilen verilerin istatistiksel olarak yorumlanması ve değerlendirilmesini gerçekleştirmişlerdir.

CONFLICT OF INTEREST (ÇIKAR ÇATIŞMASI)

There is no conflict of interest in this study.

Bu çalışmada herhangi bir çıkar çatışması yoktur.

REFERENCES (KAYNAKLAR)

[1] Redline S. Sleep and cardiovascular health: An introduction to the series. Circulation Research. 2025; 137: 705–708.

[2] Vitale GJ, Capp K, Ethridge K, Lorenzetti MS, Jeffrey M. Sleep apnea and the brain: Neurocognitive and emotional considerations. Journal of Sleep Disorders and Management. 2016; 2: 8–12.

[3] Kim DH, Kim B, Han K, Kim SW. The relationship between metabolic syndrome and obstructive sleep apnea syndrome: A nationwide population-based study. Scientific Reports. 2021; 11: 8751.

[4] Alterki A, Abu-Farha M, Al Shawaf E, Al-Mulla F, Abubaker J. Investigating the relationship between obstructive sleep apnoea, inflammation and cardio-metabolic diseases. International Journal of Molecular Sciences. 2023; 24: 6807.

[5] Javaheri S, Barbe F, Campos-Rodriguez F, Dempsey JA, Khayat R, Javaheri S, et al. Sleep apnea: Types, mechanisms, and clinical cardiovascular consequences. Journal of the American College of Cardiology. 2017; 69: 841–858.

[6] Guilleminault C, Tilkian A, Dement WC. The sleep apnea syndromes. Annual Review of Medicine. 1976; 27: 465–484.

[7] Fathima S, Ahmed M. Sleep apnea detection using EEG: A systematic review of datasets, methods, challenges, and future directions. Annals of Biomedical Engineering. 2025; 53: 1043–1067.

[8] Khandoker AH, Karmakar CK, Palaniswami M. Comparison of pulse rate variability with heart rate variability during obstructive sleep apnea. Medical Engineering & Physics. 2011; 33: 204–209.

[9] Osa-Sanchez A, Ramos-Martinez-de-Soria J, Mendez-Zorrilla A, Ruiz IO, Garcia-Zapirain B. Wearable sensors and artificial intelligence for sleep apnea detection: A systematic review. Journal of Medical Systems. 2025; 49: 66.

[10] Malhotra RK. AASM scoring manual 3: A step forward for advancing sleep care. Journal of Clinical Sleep Medicine. 2024; 20: 835–836.

[11] Lin WC, Hsu TW, Hsu CH, Lu CH, Chen HL. Alterations in sympathetic and parasympathetic brain networks in obstructive sleep apnea. Sleep Medicine. 2020; 73: 135–142.

[12] Bhongade A, Gandhi TK. Automatic identification of obstructive sleep apnea using multimodal features. Biomedical Signal Processing and Control. 2025; 105: 107609.

[13] Janbakhshi P, Shamsollahi MB. Sleep apnea detection from single-lead ECG using EDR-based features. IRBM. 2018; 39: 206–218.

[14] Yu X, Guan L, Su P, Zhang Q, Guo X, Li T, et al. OSA screening in elderly hypertensive patients using single-lead wearable ECG. Sleep and Breathing. 2024; 28: 2445–2456.

[15] Wiemers MC, Laufs H, von Wegner F. Frequency analysis of EEG microstate sequences in wakefulness and NREM sleep. Brain Topography. 2024; 37: 312–328.

[16] Dingli K, Assimakopoulos T, Fietze I, Witt C, Wraith PK, Douglas NJ. Electroencephalographic spectral analysis in sleep apnea patients. European Respiratory Journal. 2002; 20: 1246–1253.

[17] Gutiérrez-Tobal GC, Gomez-Pilar J, Kheirandish-Gozal L, Martín-Montero A, Poza J, Álvarez D, et al. Pediatric sleep apnea: Overnight

EEG as a phenotypic biomarker. Frontiers in Neuroscience. 2021; 15: 644-697.

[18] Attar ET. Detailed evaluation of sleep apnea using HRV with ML/statistical methods. Frontiers in Neurology. 2025; 16: 1636983.

[19] Han H, Seong MJ, Hyeon J, Joo E, Oh J. Classification and automatic scoring of arousal intensity using ML. Scientific Reports. 2024; 14: 5983.

[20] Malinowska U, Durka PJ, Blinowska KJ, Szelenberger W, Wakarow A. Micro- and macrostructure of sleep EEG. IEEE Engineering in Medicine and Biology Magazine. 2006; 25: 26–31.

[21] Agarwal R. Automatic detection of micro-arousals. Proc. IEEE EMBC. 2006; 1158–1161.

[22] Ferini-Strambi L, Bianchi A, Zucconi M, Oldani A, Castronovo V, Smirne S. CAP impact on HRV in young healthy adults. Clinical Neurophysiology. 2000; 111: 99–101.

[23] Chouvarda I, Mendez MO, Rosso V, Bianchi AM, Parrino L, Grassi A, et al. Predicting EEG complexity from sleep structure. Physiological Measurement. 2011; 32: 1083.

[24] Mullins AE, Jong W, Kim J, Keith W, Wong KH, Bartlett DJ, et al. Sleep EEG microstructure and neurobehavioral impairment in OSA. Sleep and Breathing. 2021; 25: 347–354.

[25] D'Rozario AL, Cross NE, Vakulin A. Quantitative EEG in adult OSA. Sleep Medicine Reviews. 2017; 36: 29–42.

[26] Appleton SL, Vakulin A, D'Rozario A. Quantitative EEG in REM/NREM associated with AHI. Sleep. 2019; 42: 6.

[27] Guzik P, Piskorski J, Awan K. Heart rate asymmetry microstructure in OSA. Clinical Autonomic Research. 2013; 23: 91–100.

[28] Li N, Wang J, Wang D, Wang Q, Han F, Jyothi K, et al. Sleep microstructure correlation with cognitive function in OSA. European Archives of Oto-Rhino-Laryngology. 2019; 276: 3525–3532.

[29] Bahr-Hamm K, Koirala N, Hanif M, Gouveris H, Muthuraman M. Sensorimotor cortical activity during arousals in OSA. International Journal of Molecular Sciences. 2023; 24: 47.

[30] Sharma M, Yadav A, Tiwari J, Karabatak M, Yildirim O, Acharya UR. Wavelet-based sleep scoring model using EEG/EMG/EOG. International Journal of Environmental Research and Public Health. 2022; 19: 7176.

[31] Šušmáková K. Human sleep and EEG. Measurement Science Review. 2004; 4: 59–74.

[32] Khandoker AH, Gubbi J, Palaniswami M. Automated scoring of OSA events using ECG. IEEE Transactions on Information Technology in Biomedicine. 2009; 13: 1057–1067.

[33] Berry RB, Brooks R, Gamaldo CE, Harding SM, Marcus C, Vaughn BV. AASM Manual for Scoring of Sleep and Associated Events. American Academy of Sleep Medicine. 2012.

[34] Chen SW, Chen HC, Chan HL. Real-time QRS detection with moving average and wavelet. Computer Methods and Programs in Biomedicine. 2006; 82: 187–195.

[35] Kadbi MH, Hashemi J, Mohseni HR, Maghsoudi A. Classification of ECG arrhythmias. Proc. MEDSIP. 2006; 398–400.

[36] Pagani J. Detection of OSA in children using pulse transit time. Computers in Cardiology. 2002; 29: 529–532.

[37] Pitson DJ, Sandell A, Van Den Hout R, Stradling JR. Pulse transit time as inspiratory effort index in OSA. European Respiratory Journal. 1995; 8: 1669–1674.

[38] Rangayyan RM. Biomedical Signal Analysis. John Wiley & Sons. 2015.

[39] Hamila R, Astola J, Alaya CF, Gabbouj M, Renfors M. Teager energy and ambiguity function. IEEE Transactions on Signal Processing. 1999; 47: 260–262.

[40] Arzeno NM, Deng ZD, Poon CS. First-derivative QRS detection algorithms analysis. IEEE Transactions on Biomedical Engineering. 2008; 55: 478–484.

[41] Seena V, Yomas J. Feature extraction and denoising of ECG using wavelet transform. Proc. IEEE Int. Caracas Conf. 2014; 1–6.

[42] Takalo R, Hytti H, Ihalainen H. Tutorial on univariate autoregressive spectral analysis. Journal

of Clinical Monitoring and Computing. 2006; 20: 379.

[43] Hjorth B. EEG analysis based on time domain properties. Electroencephalography and Clinical Neurophysiology. 1970; 29: 306–310.

[44] Hjorth B. Physical significance of time domain EEG descriptors. Electroencephalography and Clinical Neurophysiology. 1973; 34: 321–325.

[45] Pal S, Mitra M. MI detection via supervised classification. Proc. ACT Int. Conf. 2009; 398–400.

[46] Binnie CD. Computer-assisted interpretation of EEGs. Electroencephalography and Clinical Neurophysiology. 1978; 45: 575–585.

[47] Subha DP, Joseph PK, Acharya R, Lim CM. EEG signal analysis: A survey. Journal of Medical Systems. 2010; 34: 195–212.

[48] Motamedi-Fakhr S, Moshrefi-Torbati M, Hill M, Hill CM, White PR. Signal processing techniques for sleep EEG. Biomedical Signal Processing and Control. 2014; 10: 21–33.

[49] Garg G, Behl S, Singh V. PSD estimation for seizure detection. Journal of Computers. 2011; 6: 160–163.

[50] Welch PD. FFT for power spectra estimation. Digital Signal Processing. 1975; 1: 532–574.

[51] Alkan A, Yilmaz AS. Frequency domain analysis using Welch and Yule–Walker AR methods. Energy Conversion and Management. 2007; 48: 2129–2135.

[52] Collomb C. Burg's method: Algorithm and recursion. Computer Science Technical Report. 2009.

[53] Dijk DJ, Brunner DP, Beersma DGM, Borbély AA. EEG power density and slow-wave sleep vs circadian phase. Sleep. 1990; 13: 430–440.

[54] Kocak O, Ficici C, Firat H, Telatar Z. Structural EEG signal analysis for sleep apnea classification. Biomedical Engineering/Biomedizinische Technik. 2024; 69: 419-430.